

Curing Kinetics and Thermal Properties of Vinyl Ester Resins

WAYNE D. COOK,¹ GEORGE P. SIMON,¹ PETER J. BURCHILL,² MICHELLE LAU,² TRAVIS J. FITCH¹

¹ Cooperative Research Centre (CRC) for Polymer Blends, Department of Materials Engineering, Monash University, Clayton, VIC, Australia, 3168

² CRC for Polymer Blends, D.S.T.O., A.M.R.L., PO Box 4331, Melbourne, VIC, Australia, 3001

Received 13 June 1996; accepted 26 October 1996

ABSTRACT: The curing kinetics of dimethacrylate-based vinyl ester resins were studied by scanning and isothermal DSC, gel time studies, and by DMTA. The rate of polymerization was raised by increased methyl ethyl ketone peroxide (MEKP) concentration but the cocatalyst, cobalt octoate, retarded the reaction rate, except at very low concentrations. By contrast, the gel time was reduced for all increases in either peroxide or cobalt concentration. This contradictory behavior was explained by a kinetic scheme in which the cobalt species play a dual role of catalyzing the formation of radicals from MEKP and of destroying the primary and polymeric radicals. The scanning DSC curves exhibited multiple peaks as observed by other workers, but in the present work, these peaks were attributed to the individual influence of temperature on each of fundamental reaction steps in the free radical polymerization. Physical aging appeared to occur during the isothermal polymerization of samples cured below the "fully cured" glass transition temperature (T_g). For these undercured materials, the difference between the DSC T_g and the isothermal curing temperature was approximately 11°C. Dynamic mechanical analysis of a partially cured sample exhibited anomalous behavior caused by the reinitiation of cure of the sample during the DMTA experiment. For partially cured resins, the DSC T_g increased monotonically with the degree of cure, and this dependence was fitted to an equation related to the Couchman and DiBenedetto equations. © 1997 John Wiley & Sons, Inc. *J Appl Polym Sci* **64**: 769–781, 1997

Key words: vinyl ester resins; curing kinetics; glass transition; DSC; DMTA

INTRODUCTION

Vinyl ester resins are formed by the copolymerization of styrene monomer and a dimethacrylate monomer based on the diglycidyl ether of bisphenol-A (see Fig. 1). Their resistance to degradation by corrosive and hostile environments leads to their use in many applications, such as in swimming pools, sewer pipes, and solvent storage tanks, and thus, vinyl ester resins are of considerable commercial interest.¹

Despite their increasingly widespread usage,

the interrelationship between their chemistry, reaction kinetics, morphology, and properties is not well understood because of the complexity of their formulation. For example, the nature of the copolymerization of the styrene and dimethacrylate monomers and the resulting morphology could be influenced by reaction conditions such as temperature and initiator concentrations. Previous studies of these materials have investigated the curing behavior of vinyl ester resins^{2,3} and their chemorheology⁴ and have related their mechanical properties⁵ to the cured structure. Infrared and ¹³C-NMR studies^{6,7} of the cure of vinyl ester resins have indicated that the polymerization is initially random, but that as cure progresses, styrene homopolymerization tends to dominate and, on com-

Correspondence to: Wayne D. Cook.

Contract grant sponsor: CRC for Polymer Blends.

© 1997 John Wiley & Sons, Inc. CCC 0021-8995/97/040769-13

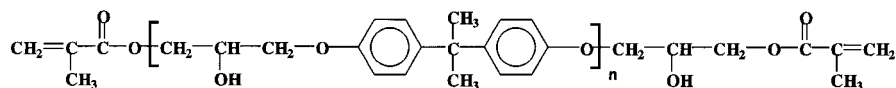


Figure 1 Structure of monomer system.

pletion of the reaction, significant amounts of unreacted methacrylate can be found. The properties of the cured resin appear to depend⁸ on the initiator system, but no in-depth study of the mechanism appears to have been made. In the present study, an understanding is sought for the manner in which the initiation system and curing temperature controls the polymerization kinetics and, thus, the final extent of cure and glass transition temperature of the network via the underlying structure.

EXPERIMENTAL

The vinyl ester resin used in this study, Hetron 922, was supplied by Huntsman Chemical Company, Australia. This resin contains approximately 45 wt % styrene and 55 wt % of a dimethacrylate based on an oligomerized diglycidyl ether of bisphenol-A. The molecular weight of the dimethacrylate is approximately 1080, and its generic structure is shown in Figure 1. When $n = 1$ in Figure 1, the resin is known as bisGMA or bisphenol-A diglycidyl methacrylate. In the present study, the resin was usually used as a two-component system with part A containing vinyl ester resin and varying amounts of MEKP (methyl ethyl ketone peroxide as a 40 wt % solution in dimethylphthalate), and part B containing vinyl ester resin and varying amounts of cobalt-II octoate (as a 6 wt % solution of cobalt in white oil). These two components were stored at 4°C until required and were mixed in equal parts to initiate the reaction. In the mixed and activated resin, the concentration of MEKP solution varied from 0 to 2.4 wt % (1.2 wt % was the standard level, equivalent to 0.48 wt % of pure MEKP) and the concentration of the cobalt-II solution ranged from 0 to 3.2 wt % (0.2 wt % was the standard level, equivalent to 0.012 wt % Co-II). In some cases the activated resin was prepared in one stage by dissolving the required quantity of cobalt salt solution in the resin and then adding the requisite MEKP solution and rapidly stirring the mixture. In this article, all descriptions of cobalt and MEKP concentrations are expressed as wt % of the catalyst

or MEKP solutions mixed into the vinyl ester resin.

The kinetics were monitored on a Perkin-Elmer DSC-7, using both isothermal and scanning (10°C/min) modes, in sealed aluminium pans with a sample mass in the range of 10–15 mg. In some cases, the Perkin-Elmer Intracooler was also used for subambient runs. The data was converted from heat flow (dq/dt in W) to fractional conversion rate ($d\alpha/dt$ in min^{-1}) by use of the expression:

$$d\alpha/dt = (dq/dt)/m \cdot \Delta H_p, \quad (1)$$

where m is the sample mass (in g) and ΔH_p is the total heat of polymerization. The heat of polymerization has been determined to be 67.4 kJ/mol by Tong and Kenyon⁹ for styrene and to be 57.8 kJ/mol¹⁰ for methyl methacrylate. Thus, a simple molar average for the vinyl ester resin would be 65.5 kJ/mol. A better estimate can be obtained by interpolation of the copolymerization data of Suzuki et al.¹¹ for styrene/methyl methacrylate. This yields a value of 67.3 kJ/mol (360 J/g) for the monomer composition in the vinyl ester resin, and this value was used for ΔH_p in eq. (1). The use of a single value of the heat of polymerization to calculate the overall rate of conversion of unsaturation in the copolymerization is justified because the styrene and methacrylate units have similar ΔH_p values and because the copolymerization of styrene with phenyl glycidyl methacrylate (which may be considered the monomeric version of the dimethacrylate in Fig. 1) has been shown to be almost random.¹² The rate data calculated from eq. (1) was integrated numerically to obtain the conversion data.

Gel times were determined at 23°C by measuring the time from the start of mixing until the first appearance of a gel as determined by a TECAM gel timer (Townson and Mercer).

The dependence of T_g on conversion was evaluated by partially curing samples in scanning mode (i.e., scanning to various predetermined temperatures), rapidly cooling and rescanning the sample through the glass transition region to determine the T_g . The dependence of T_g on curing tempera-

ture (T_{cure}) was obtained by curing the sample isothermally in the DSC until no further heat was evolved, rapidly cooling, and rescanning the sample through the glass transition region.

Dynamic mechanical thermal analysis (DMTA) of the blends was performed with double cantilever geometry using a Polymer Laboratories Mk II DMTA operated at 1 Hz and scanned at 2°C/min. Samples of vinyl ester resin were cured at 23°C for 16 h with or without a postcure at 90°C for 90 min and then were scanned as a function of temperature through the glass transition region.

RESULTS AND DISCUSSION

Reaction Scheme

Based on the steady-state assumption for radical concentration, the rate of polymerization of a monomer is given by¹³:

$$-d[M]/dt = k_p[M][M_n^*] = k_p[M]\{fR_i/k_t\}^{1/2}, \quad (2)$$

where $[M]$ and $[M_n^*]$ are the monomer and radical concentrations, f is the initiation efficiency, R_i is the rate of initiator decomposition, and k_p and k_t are the propagation and termination rate constants, respectively. For the cobalt octoate/MEKP redox system, the molar ratio of cobalt to hydroperoxide groups is approximately 0.02 for the standard levels used here. For these levels, the postulated mechanism for initiation is¹⁴:



where $R-OOH$ and Co represents the MEKP and cobalt species and k_{d1} and k_{d2} represent the rate constants for the formation of the alkoxy (RO^{\bullet}) and peroxy (ROO^{\bullet}) radicals, respectively. Beaunez et al.¹⁵ have noted that the alkoxy radical is much more reactive to ethylenic monomers than the peroxy radical and so eq. (3) determines the rate of initiation. Equation (4) is important, however, because in this step Co^{2+} is regenerated, which results in a pseudosteady state for the Co^{2+} concentration. As a result, the rate of formation of alkoxy radicals is predicted to be approximately constant until the MEKP concentration is se-

verely depleted as indicated by the reaction kinetics:

$$d[RO^{\bullet}]/dt = k_{d1}[Co^{2+}][R-OOH]. \quad (5)$$

Assuming that a steady state exists for the formation of Co^{2+} , the equilibrium concentration of Co^{2+} is thus:

$$[Co^{2+}] = k_{d2}[Co^{2+}]_o/(k_{d1} + k_{d2}), \quad (6)$$

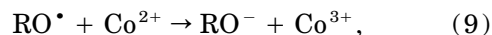
where $[Co^{2+}]_o$ is the initial cobalt octoate concentration. Thus, the rate of initiation is given by:

$$R_i = k_{d1}k_{d2}[R-OOH][Co^{2+}]_o/(k_{d1} + k_{d2}). \quad (7)$$

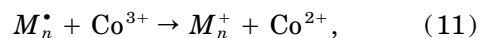
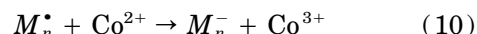
Combination of eq. (7) with eq. (2) indicates that the rate of polymerization should increase with increased cobalt and MEKP levels:

$$\frac{d[M]}{dt} = k_p[M] \left(\frac{fk_{d1}k_{d2}[R-OOH][Co^{2+}]_o}{k_t(k_{d1} + k_{d2})} \right)^{1/2}. \quad (8)$$

In practice, the above scheme is complicated by the fact that commercial MEKP consists of several different peroxide molecules of differing reactivities.¹⁶ In addition, the initiating radicals may themselves be consumed by side reactions such as reduction by Co^{2+} .¹⁴



and the propagating radicals may be lost by similar side reactions¹⁷:



which further complicate the kinetics.

Effect of Initiator Concentration

To investigate the curing kinetics, the vinyl ester resin was cured in scanning mode using various MEKP/Co octoate ratios. Figure 2 shows the effect of MEKP on the cure and indicates that with an increase in the MEKP concentration, the exotherm peak (corresponding to the maximum reaction rate) is shifted to lower temperature as would be expected for a faster reacting system.

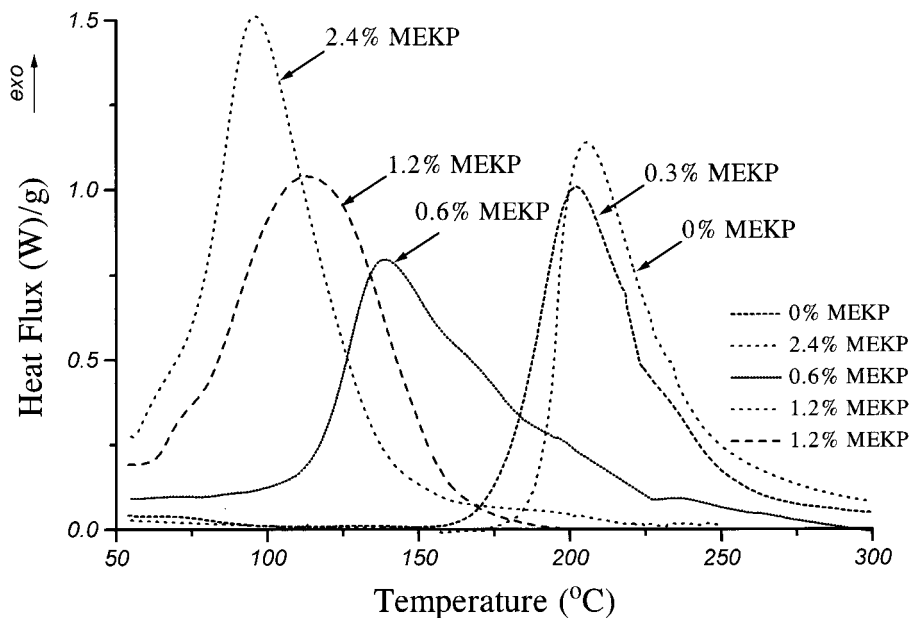


Figure 2 Heat flux vs. temperature using 0.2 wt % cobalt octoate solution and varying levels of MEKP solution.

This is consistent with the prediction of eq. (8), which shows that the rate should increase as the peroxide concentration is raised. The effect of MEKP concentration on the isothermal kinetics at 70°C is shown in Figure 3. In some cases, a small maximum (or shoulder) was also observed

in the early stages of the reaction (less than 5 min), prior to the major exotherm due to the main reaction process. This initial maximum is probably due to small traces of H_2O_2 because H_2O_2 is a known MEKP contaminant³ that reacts with the cobalt catalyst to form radicals more readily than

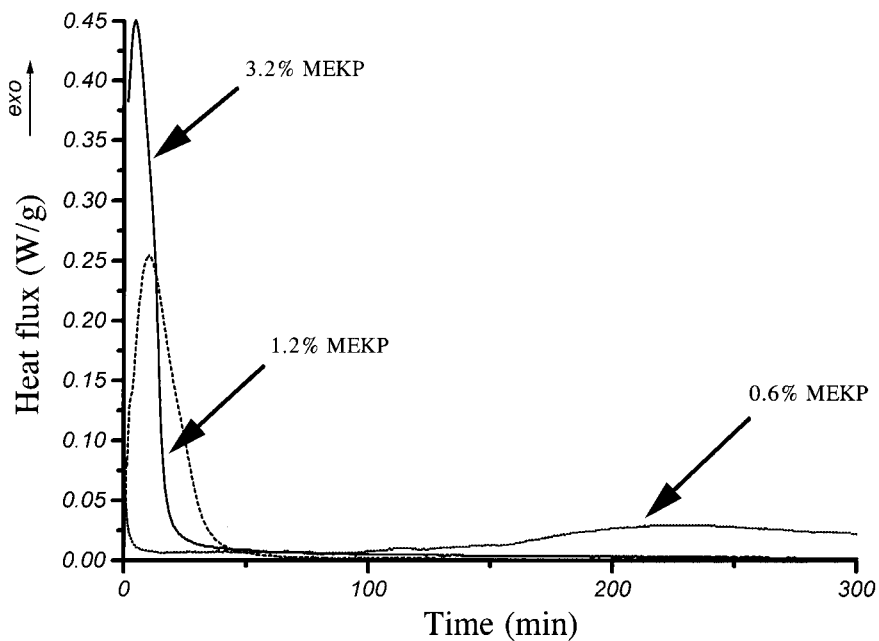


Figure 3 Heat flux vs. time using 0.2 wt % cobalt octoate solution and varying levels of MEKP solution at 70°C.

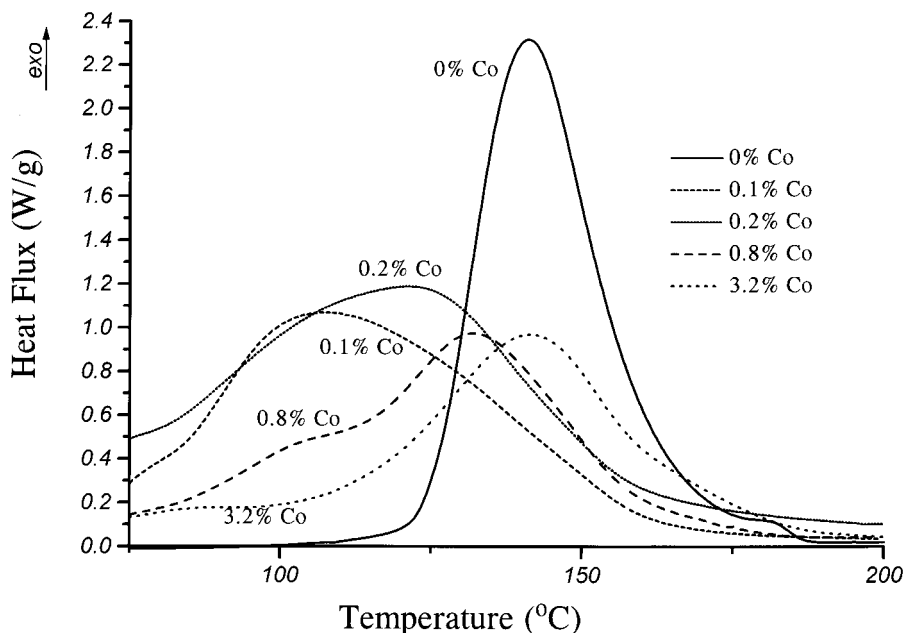


Figure 4 Heat flux vs. temperature using 1.2 wt % MEKP solution and varying levels of cobalt octoate solution.

MEKP, and this may cause the early (but limited) initiation of vinyl resins.³ Even though the reaction is accelerated by increasing MEKP concentration (Figs. 2 and 3), the dependence of rate on concentration is not in accord with eq. (8) because the maximum isothermal rate obtained from the data in Figure 3 is not proportional to $[R-OOH]^{1/2}$ but, in fact, is approximately proportional to $[R-OOH]^{3/2}$.

Figure 4 illustrates the effect of varying the cobalt octoate concentration on the DSC traces. It is surprising to note that with the exception of very low levels (≤ 0.1 wt %), the exothermic maximum in the DSC trace (corresponding to the maximum rate) occurs at higher temperatures as the cobalt octoate concentration is raised, suggesting that the cobalt salt actually retards the reaction. Similar results have been observed by Salla et al.,¹⁸ as discussed below. Figure 5 shows the corresponding isothermal kinetics. In this data, large induction periods (20 and 140 min) were observed for the systems containing 0 and 3.2 wt % cobalt octoate, respectively. These induction periods were probably due to inhibition of the polymerization by dissolved trace oxygen or by the cobalt ions themselves. To aid comparison of the data in Figure 5, this induction period has been subtracted from the time axis in each graph. The data in Figure 5 indicates that at intermediate catalyst levels, an increase in the Co^{2+} concentration re-

sults in a reduction in the rate of polymerization, in agreement with the scanning DSC data, but in conflict with the proposed mechanism [eq. (8)].

The time for gelation is very important to the resin application because it gives an indication of the working time of the resin, which in turn, can be manipulated by variation in the concentration of the initiator.¹⁴ Figure 6 shows the gel time vs. the MEKP or cobalt salt concentration. In this figure, an increase in the MEKP concentration is seen to reduce the gel time, which is in agreement with gel time results of other workers¹⁴ and the above kinetic scheme [eq. (8)]. On the assumption that the gel time is reciprocally related to the reaction rate, these results are also consistent with the observed accelerating influence of MEKP on the polymerization rate (Figs. 2 and 3).

The data in Figure 6 also shows that increasing the cobalt salt concentration also reduces the gel time, whereas cobalt was found to decelerate the rate in the DSC studies (Figs. 4 and 5). The gel time data shown in Figure 6 is similar to that reported by Kamath and Gallagher¹⁴ for the curing of unsaturated polyester resins; however, Cassoni et al.¹⁹ found that the gel time showed very little dependence on Co^{2+} concentration within the range 0.2–0.8 wt % of cobalt salt solution (for cobalt solutions of the same strength as in the present work) in vinyl ester resins. The reasons for the different effects of cobalt concentration on

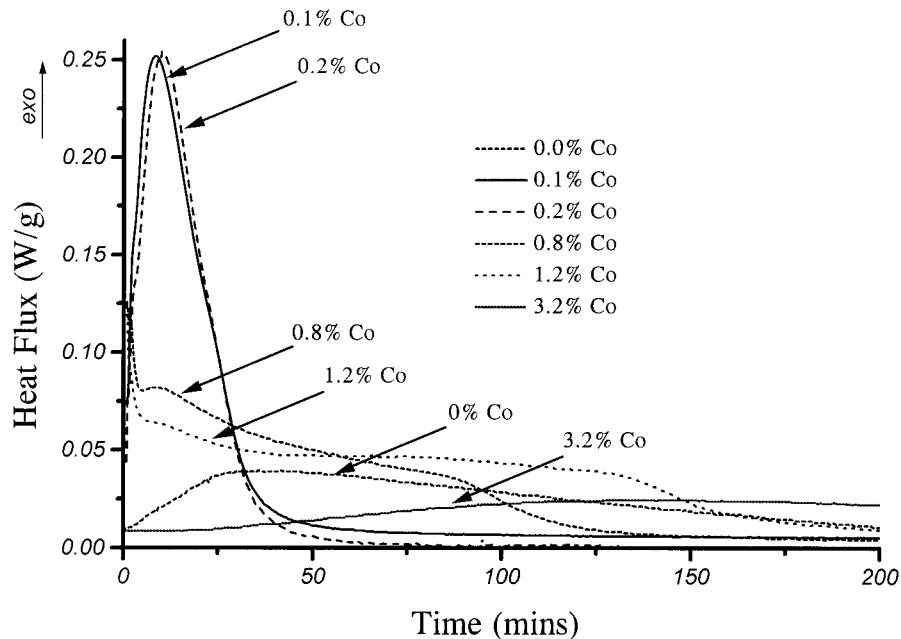


Figure 5 Heat flux vs. time using 1.2 wt % MEKP solution and varying levels of cobalt octoate solution at 70°C. To aid comparison of the data, the induction periods have been subtracted from the time axis for the samples with 0 and 3.2 wt % cobalt octoate solution.

the gel time (Fig. 6) and reaction rate (Figs. 3 and 5) are not readily apparent. It is expected that the gel time should be inversely related to the reaction rate because the gel point corresponds to the first formation of an infinite network, and this usually occurs at a fixed conversion for the particular resin system.²⁰ It could be argued that the above interpretation is in error because an increase in initiator level will decrease the kinetic

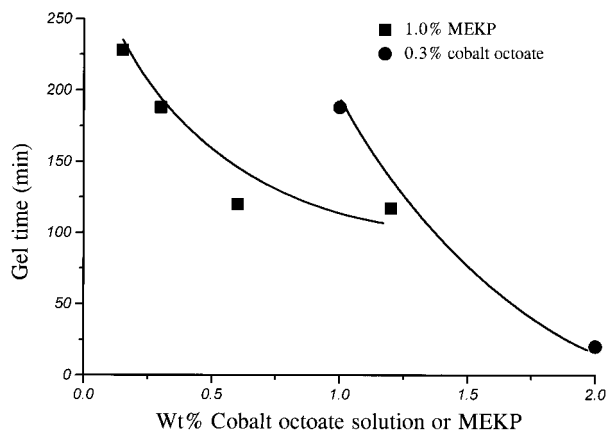


Figure 6 Gel time vs. concentration of cobalt octoate solution at a constant 1.0 wt % MEKP concentration (squares) or vs. concentration of MEKP solution at a constant 0.3 wt % cobalt octoate concentration (circles).

chain length¹³ and retard the gel point, thus affecting the time to gel. However, both the reciprocal gel time and the reaction rate increase with increasing MEKP concentration, so that these results do not support this idea. Because the gel point for the current vinyl ester resins is expected to be only a few percent (by comparison with the data for other vinyl/divinyl systems²¹), it is possible that cobalt salts accelerate the reaction in the initial stages encompassing the gelation process, but at higher extents of conversion, which are more clearly observed in the reaction rate studies by DSC, the metal acts as a retarder. This inhibition role could be manifest in eq. (9) where the alkoxy radical is destroyed or in eqs. (10) and (11) where the methacrylate or styryl radical are deactivated by cobalt salts.

The scanning calorimetry traces shown in Figures 2 and 4 appear to be composed of at least two exothermic peaks that vary in size and position as the concentrations of MEKP and cobalt octoate are altered. This indicates that the polymerization kinetics are quite complicated and suggests the occurrence of two separate reaction processes. These observations are also supported by the isothermal kinetic studies most clearly shown in Figure 5 where the reaction rate curve appears to be the superposition of two curves and so is sugges-

tive of two reaction processes. Avella et al.²² have also noted multiple peaks in the scanning DSC of Co^{2+} /MEKP-initiated styrene/unsaturated polyester resins and suggested that the first peak was due the copolymerization of the styrene with the polyester fumarate unsaturation, while the latter was caused by styrene homopolymerization. The results in Figures 2–5 are not consistent with this interpretation unless variations in initiator concentration can drastically alter the copolymerization process. Salla et al.¹⁸ also studied the curing kinetics for unsaturated polyester resins by varying the cobalt octoate concentration. In their investigation, Salla et al.¹⁸ attributed the lower temperature peak to polymerization initiated by the redox pair and the second, higher temperature peak to polymerization initiated by the uncatalyzed decomposition of MEKP. A similar interpretation was made by Lem and Han² in studies on vinyl ester resins and polyester resins. The data in Figures 2 and 4 are not consistent with the reaction scheme of Salla et al.¹⁸ For the systems where the MEKP concentration is varied (Fig. 2), the lower temperature peak (which is supposedly due to the redox initiated polymerization¹⁸) is maximized by a high ratio of peroxide to catalyst, whereas the upper peak (attributed to homolytic fission of the MEKP¹⁸) is largest for low ratios of MEKP to cobalt. For the systems where the Co^{2+} concentration is varied (Fig. 4), the high temperature peak is dominant at both high and low catalyst concentrations but not for intermediate levels. Thus both observations are contrary to the proposed mechanism of Salla et al.¹⁸

It should be noted that multiple exothermic peaks have also been reported in isothermal studies of the peroxide-initiated polymerization of styrene/MMA²³ and in the photochemical homopolymerization of dimethacrylates,²⁴ even though only one initiation system is present, and it has been suggested²⁴ that this is caused by complex variations in k_p and k_t [eq. (8)]. Thus, the apparently anomalous data shown in Figures 2 and 4 may be due to the complex variation in rate constants as the polymerization proceeds (for isothermal cure) and in addition when the temperature is varied in scanning experiments.

Effect of Cure Temperature

To further investigate the curing kinetics, the vinyl ester resin was isothermally cured at a range of temperatures but with constant initiator concentration. Figure 7 shows the rate as a function

of the degree of conversion for a range of isothermal cure temperatures. As discussed earlier, in the early stages of the reaction, small peaks were observed which may be caused by the H_2O_2 impurity in the MEKP.³ In most cases, the initial maximum is followed by a broader maximum in the reaction rate. This appearance of a rate maximum and the general variation of the rate during cure is not uncommon and is generally observed in free radical polymerizations of divinyl monomers as a result of diffusional influences on the kinetic steps.^{25–28} At low conversions, termination of chain radicals occurs by chain translation or segmental diffusion. However as the polymerization proceeds, a gel structure develops which, in the present system, is expected to occur after a few percent reaction.²¹ This three-dimensional gel restricts the diffusion of the long chain radicals, thus dramatically slowing bimolecular termination. As a result, eq. (8) predicts that the polymerization rate should rise producing the Tromsdorff or gel effect.¹³ When the segmental mobility is reduced by further reaction, another termination mechanism known as “reaction diffusion” starts to dominate. In this process, two radicals are brought into proximity by a series of propagation steps, thus enabling termination. Because reaction diffusion is less sensitive to changes in molecular mobility, the rate constant for termination approaches constancy. However, the decreased mobility also leads to a reduction in the rate of primary radical diffusion from the radical cage, resulting in a decrease in initiation efficiency.²⁸ The near-constancy of k_t and the reduction in initiation efficiency (f) thus causes a maximum in the overall rate of reaction. As the network continues to develop, the increased crosslinking may even reduce the mobility of the monomers causing a reduction in propagation rate and thus a further decline in overall rate. In the final stages of reaction, the depletion of monomer will also lower the polymerization rate.

The data in Figure 7 are in general agreement with the kinetic scheme discussed above. For low curing temperatures, the rate is initially low but it passes through a broad maximum as the reaction proceeds. The reaction then slows and finally ceases before all of the monomer has been consumed. The cessation of polymerization prior to total monomer consumption has been widely observed in the cure of glass-forming networks^{23,26,29} and is due to diffusion control of the curing process when the glass transition temperature (T_g) approaches the curing temperature (T_{cure}). At

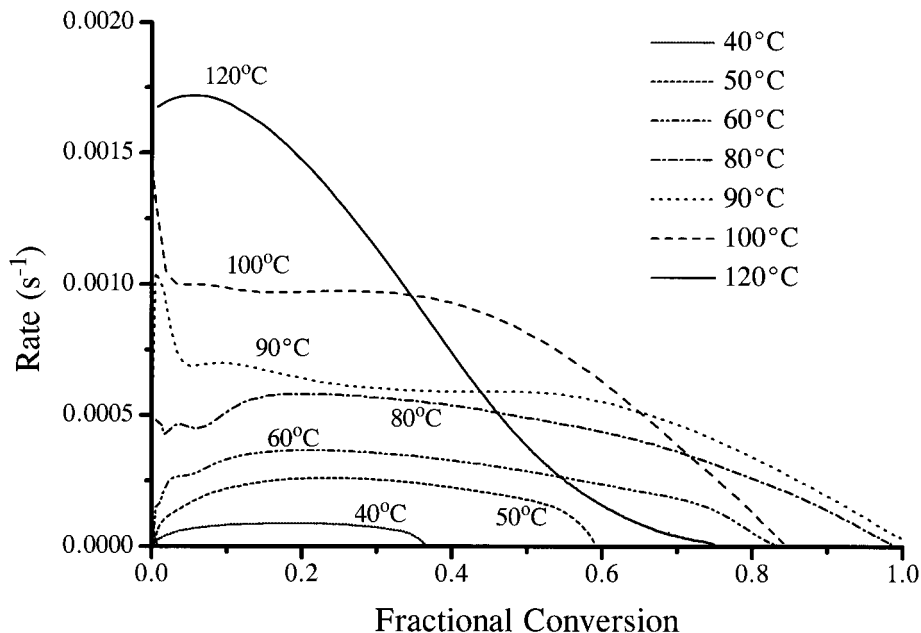


Figure 7 Conversion rate ($d\alpha/dt$) vs. conversion at various isothermal temperatures, using 1.2 wt % MEKP solution and 0.2 wt % cobalt octoate solution.

higher curing temperatures, the final degree of cure is increased because the material can polymerize further before the T_g rises above T_{cure} . As indicated in Figure 7, when the curing temperature is between 80 and 90°C, the final degree of conversion is relatively constant and the system is close to complete cure. However, at the highest curing temperatures (100 and 120°C), the final degree of cure appears to be lower than that found at the intermediate curing temperatures. This may result from partial degradation of the network caused by depolymerization of the dimethacrylate, as has been suggested for similar dimethacrylates elsewhere.²⁶ Alternatively, at the high curing temperatures, the accelerated decomposition of the initiator may result in its total consumption prior to full polymerization of monomer. This phenomenon is known as “dead end polymerization”³⁰ and can result in lower degrees of conversion than anticipated.

Curing and Physical Aging

During their cure in bulk, vinyl ester resins undergo an exotherm and so it is instructive to study how the cure temperature (T_{cure}) determines the degree of cure and the resulting T_g . The dependence of T_g on the curing temperature (T_{cure}) was obtained by curing samples of the resin isothermally in the DSC until there was no further sign

of reaction (over a period of 6 h). The sample was then cooled rapidly (at ca. 100°C/min) to below 0°C and subsequently scanned up through the glass transition region. The DSC traces obtained during this rescan are shown in Figure 8. Samples cured isothermally below the maximally attainable T_g ($\leq 100^\circ\text{C}$) were found to exhibit an endothermic maximum in the glass transition region, whereas samples that had been isothermally cured above 100°C exhibited the classic sigmoidal shape of the heat capacity curve (see Fig. 8). Also included in Figure 8 are DSC traces on samples that had been partially cured by scanning up to a certain temperature, rapidly cooled and rescanned to determine the T_g . In each of these cases, no maximum is observed in the second DSC scan until well after the glass transition region where additional polymerization caused an exotherm.

The maximum observed in Figure 8 for the isothermally cured samples (e.g., the sample isothermally cured at 40°C) may result from the superposition of the heat capacity step of the T_g with an exothermic peak (due to further reaction) and this could cause a minimum shortly after the glass transition. In addition, the maxima in the transition region may also be associated with physical aging during cure.^{31–33} The cause of aging and its effect on the DSC traces can be understood as follows. If a sample is isothermally cured at a tem-

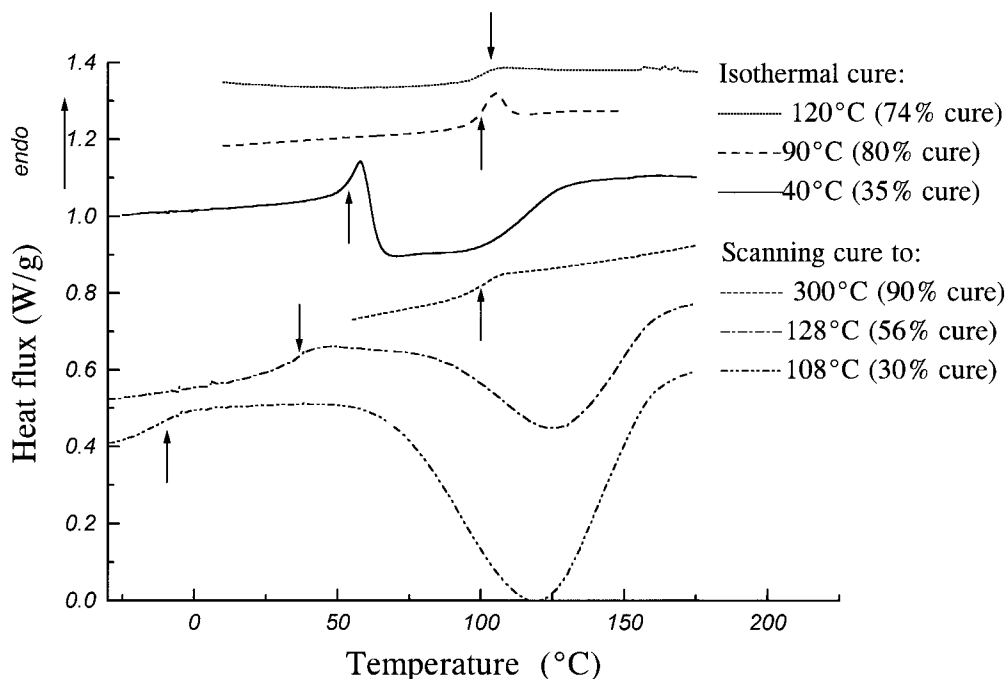


Figure 8 Heat flux vs. temperature in the glass transition region (indicated by arrows). In the top group, the resins were cured isothermally at the indicated temperatures (resulting in the indicated degree of cure) and were then rescanned as shown by the DSC trace. In the lower group, the samples were scanned up to the indicated temperature (at 10°C/min, resulting in the degree of cure as indicated) and were then rescanned as shown by the DSC trace.

perature above its maximal T_g , the material remains in the liquid-like state during cure and the enthalpy of the system is at its equilibrium value. As a result, when this sample is rapidly cooled through the T_g and then heated, the enthalpy exhibits a change in gradient at the T_g and the heat capacity (the derivative of enthalpy with respect to temperature) undergoes a sigmoidal shaped increase. However, if the sample vitrifies during cure and remains in this glassy state for several hours, the sample may age by slow segmental motion. If this sample is then cooled and rescanned, the relaxation rate of the molecular segments will be too slow for the materials to reach the equilibrium state during the temperature ramp until the glass transition is reached. At this temperature, the material will rapidly adjust to the equilibrium liquid enthalpy by a rapid rise. As the temperature is further raised, the enthalpy will show a more steady rate of increase associated with the liquid state. As a result, the enthalpy passes through a step and the heat capacity exhibits a maximum superimposed on the classic sigmoidal step-like curve. In contrast, samples cured by the scanning method never vitrify during the temper-

ature ramp and so do not have an opportunity to undergo physical aging and thus exhibit only the classic sigmoidal shaped curve.

Effect of Cure Temperature on T_g

Figure 9 indicates that for isothermally cured samples, the difference between T_g and T_{cure} is

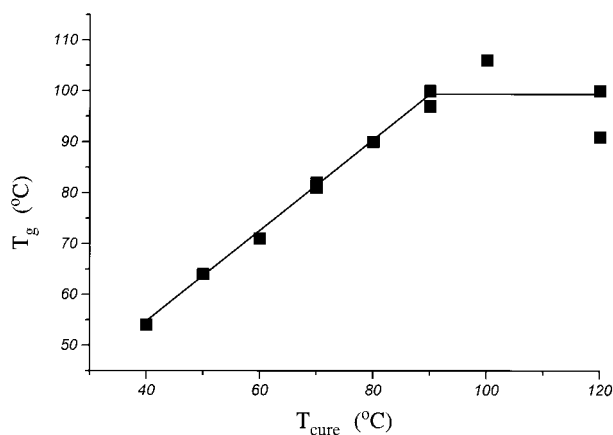


Figure 9 T_g obtained by DSC versus isothermal cure temperature (T_{cure}).

constant (and equal to ca 11°C) up to 80°C, and at higher cure temperatures the T_g is approximately constant (ca 100°C). Similar results have been obtained for epoxy resin cure^{29,31–33} where the difference between the DSC T_g and T_{cure} has been found to range from 10 to 30°C. Tungare and Martin³⁴ have investigated this issue with DSC studies of bismaleimide resin cure and found that, in this case, $T_g - T_{\text{cure}}$ ranges between 4 and 23°C. When dynamic mechanical spectroscopy (at 1 Hz) is used to characterize the glass transition in epoxy resins, the T_g defined by the inflection in the modulus has been found to be from 15 to 30°C higher than the curing temperature³³ while the T_g defined by the $\tan \delta$ maximum is 20 to 70°C higher than T_{cure} .³⁵ Similarly, Kloosterboer and Lijten³⁶ found the difference between the T_g ($\tan \delta$) and T_{cure} to be 70°C for a diacrylate network.

It is of interest to compare the experimental difference between T_g and T_{cure} and the prediction of the theory of chemico-diffusion kinetics.²⁵ In this theory, the diffusion rate constant is expressed by the WLF equation:

$$k_{\text{diff}} = k_{\text{diff}(T_g)} \exp \left\{ \frac{2.303 c_1 (T_{\text{cure}} - T_g)}{(T_{\text{cure}} - T_g + c_2)} \right\} \quad (12)$$

where $k_{\text{diff}(T_g)}$ is the diffusion rate constant at T_g . When T_g is equated to the value determined by dilatometry (which is also close to that obtained by DSC), the average values of c_1 and c_2 are 17 and 50°C.³⁷ Equation (12) predicts that the diffusion rate tends to zero when $T_g - T_{\text{cure}}$ equals c_2 . However, for chemical reaction to occur, the reacting groups must diffuse within the collisional radius prior to reaction, so that the curing process will be completely arrested if the diffusion rate is zero. Because the average or “universal” value of c_2 is 50°, ³⁷ eq. (12) predicts that curing should cease when the T_g is 50°C above the curing temperature, rather than at the experimentally observed value of $T_g + 11^\circ\text{C}$. Three reasons can be used to explain this discrepancy. The first reason is based on the variability of c_2 . While the universal value of c_2 is 50°, experimentally it has been found to vary over the range of 20–130°C³⁷ so that cessation of cure is predicted to occur at a temperature ranging from $T_g + 20$ to $T_g + 130$, depending on the network-forming system. The second explanation relates to the time scale of the reaction kinetics experiment. When vitrification starts to occur, the curing process will be severely retarded and experimentally the reaction may ap-

pear to have ceased. However, this is only true over the time scale of the observation (approximately 6 h) so that over a much longer time scale, further reaction can occur, thus raising T_g above the experimentally determined value. Finally, it should be recognized that after isothermal curing, the material may cure further during the subsequent DSC scan, thus raising the measured T_g above the value during the isothermal cure. This effect would increase the difference between T_g and T_{cure} .

Effect of Partial Curing on DMTA

The effect of cure temperature on the dynamic mechanical properties are shown in Figure 10. For the sample cured at 23°C, the modulus and $\tan \delta$ curves appear to show two glass transitions at approximately 65 and 115°C. In contrast, the sample cured at 23°C and postcured at 90°C exhibits only one glass transition region. The anomalous behavior exhibited by the room temperature cured material has been reported for related studies of bisphenol-A based polyester resins³ and can be explained in terms of the additional cure of the sample when the temperature is being scanned in the DMTA as originally discussed by Gillham et al.³⁸ The observed behavior depends on the competition between the rate of temperature rise and the rate of cure and hence increase in T_g . Thus, prior to measurement by DMTA, the 23°C cured material was only partly cured, having vitrified during the curing process at room temperature. As the sample is heated, it enters the glass transition region. The start of the transition region (as defined by the modulus inflection) is approximately 55°C, which is 22°C higher than the cure temperature—this compares well with the 11°C difference between T_{cure} and T_g discussed above. As the temperature is raised further, the thermal energy provides sufficient molecular mobility to recommence the curing process, causing a shift in the transition region and an increase in the modulus. As the temperature is raised still further, the reaction finally ceases as the system approaches full cure. At this point, the modulus decreases again as the material passes out of the transition region and into the rubbery region. The $\tan \delta$ curve can be interpreted in a similar manner. It is interesting to note that the temperatures of the final $\tan \delta$ maxima and the values of the rubbery moduli of the two samples are very similar, indicating that both have the same final structure, independent of the cure cycle.

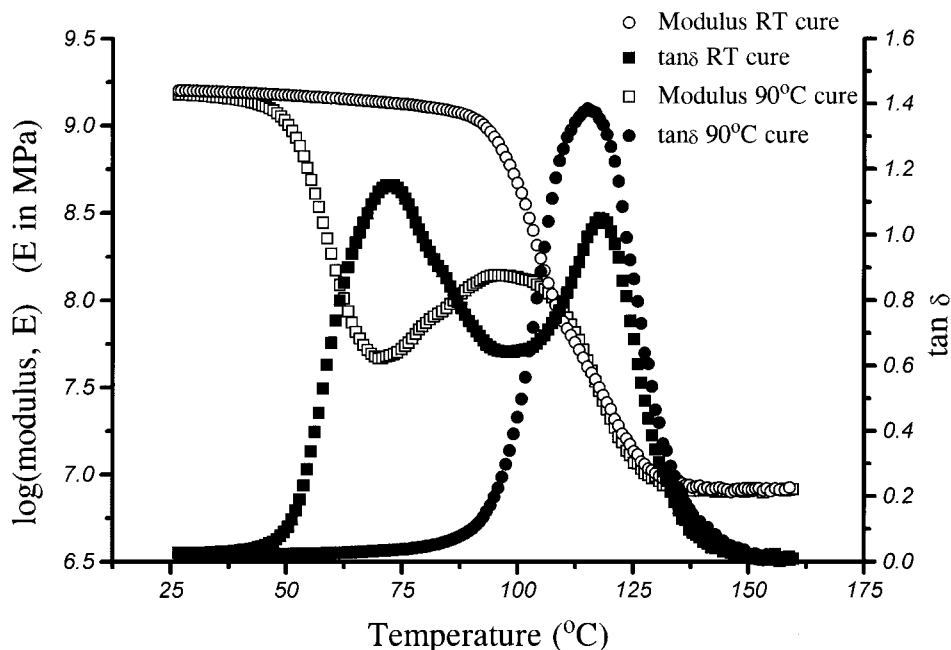


Figure 10 Flexural modulus (unfilled symbols) and $\tan \delta$ (filled symbols) vs. temperature for a vinyl ester resin cured at 23°C (squares) and for an identical sample cured at 23°C and postcured at 90°C for 1.5 h (circles).

T_g and Conversion

The relationship between the degree of conversion and the T_g is important practically for the optimum use of the material and is of theoretical interest. A number of workers have demonstrated that there is a unique relation between T_g and the degree of conversion for epoxy resins^{39–41} and for cyanate resins,⁴² which is independent of cure path, provided that secondary reactions are not significant.⁴¹ In the present study, T_g -conversion data was obtained by scanning samples in the DSC from 0°C up to a fixed temperature so that the resin was partially cured. The extent of cure was determined by integration of the partial exotherm from the start of the scan up to its termination at the upper temperature. The sample was then rapidly cooled to -50°C and rescanned at 10°C/min to give the T_g of the partially cured sample. In undercured samples, an additional exotherm occurred after this glass transition. Summation of the polymerization enthalpies of the first and second exotherms were approximately constant as expected. Figure 11 shows the dependence of T_g on the degree of conversion obtained by this technique. The resulting curve has the same positive curvature as has been found for novolac vinyl ester resins,⁴³ epoxy resins,^{39–41} ure-

thanes,⁴⁴ cyanate resins,⁴² and bismaleimides,³⁴ but the degree of curvature is less.

Pascualt and Williams⁴⁵ have recently compared the predictions of Couchman and of Di-Benedetto for the dependence of T_g on curing and have shown⁴⁵ that under certain conditions these theories have the same formalism that can be represented by the equation:

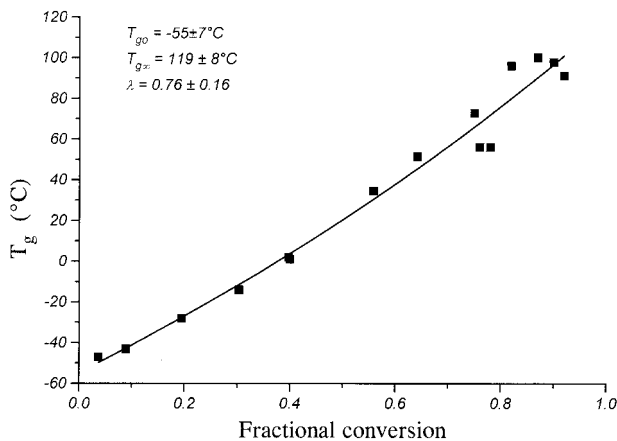


Figure 11 T_g vs. conversion for partly cured samples. The curve is the fit to the data using eq. (13).

$$\frac{(T_g - T_{g0})}{(T_{g\infty} - T_{g0})} = \frac{\lambda\alpha}{1 - (1 - \lambda)\alpha}, \quad (13)$$

where T_{g0} and $T_{g\infty}$ (in K) are the glass transition temperatures of the original uncured resin and the fully cured polymer, α is the fractional conversion and λ is a glass transition parameter. In one interpretation of the theory,⁴⁵ λ is given by:

$$\lambda = T_{g0}/T_{g\infty}. \quad (14)$$

Equation (13) was used to fit the T_g -conversion data in Figure 11. The extrapolated values of T_{g0} and $T_{g\infty}$ are -55 and 119°C , respectively. The value for λ of 0.76 obtained by fitting the data to eq. (13) is similar to but larger than the theoretical value of 0.56 obtained from the ratio $T_{g0}/T_{g\infty}$ in eq. (14).⁴⁵

CONCLUSIONS

The reaction kinetics and the relaxational behavior of a vinyl ester resin has been studied using thermal techniques as a function of cure temperature and of peroxide and cobalt catalyst concentrations. It has been found that the reaction rate (determined by DSC) was raised and the gel time reduced with increasing concentrations of MEKP. However, while the gel time was also reduced by increases in the cobalt level, the reaction rate was lowered. This was attributed to a dual nature of cobalt in the polymerization process and the differing sensitivity of the gel times and DSC data to these roles. These results caution the use of a single technique to characterize the effect of commercial additives on the cure of vinyl ester resins.

The reaction process was shown to be complex, as indicated by the presence of multiple peaks in the scanning DSC data. For the isothermal studies, an initial short term polymerization rate, attributed to H_2O_2 initiation, was followed by a broad maximum in the polymerization rate due to the Tromsdorff effect. The rate of polymerization and the final degree of reaction increased as the curing temperature was raised and then reached a maximum—at the highest temperature, the degree of cure was reduced due to degradation or premature loss of initiator.

During isothermal cure, samples appeared to exhibit physical aging when vitrification occurred during the curing process. For low and intermediate cure temperatures, the T_g was found to be 11°C above the cure temperature due to the influ-

ence of diffusion on the polymerization rate. At higher cure temperatures, the T_g approached an upper limit as a result of near-complete cure.

The role of the cure temperature in defining the T_g was also demonstrated by DMTA studies. For the sample cured at room temperature, two apparent glass transition region were exhibited in the DMTA trace but only one transition was observed for the “fully” cured sample. This anomalous behavior was explained in terms of the influence of the additional cure that occurred during the DMTA experiment.

The T_g was found to strongly depend on the degree of cure in the vinyl ester resin. The T_g -conversion relation of Pascault and Williams⁴⁵ was applied to the data and was found to give an adequate representation of experimental results.

T.F. is grateful to the CRC for Polymer Blends for scholarship support during which this work was undertaken. The authors would like to thank Dr. Carolyn Morris (DSTO), Dr. Ian Dagley, and Dr. Alastair McKee for their support of this work and Dr. Geoff Houghton and Dr. Graham Durrant (Huntsman Chemical Company) for supplying the materials.

REFERENCES

1. L. C. Muszynski, in *Encyclopedia of Polymer Science and Technology*, Vol. 12, H. F. Mark, N. M. Bikales, G. C. Overberger, and G. Menges, Eds., Wiley Publications, New York, 1988, p. 462.
2. K.-W. Lem and C. A. Han, *Polym. Eng. Sci.*, **24**, 175 (1984).
3. T. H. Grentzer, D. A. Rust, S. K. Lo, C. J. Spencer, and G. W. Hackworth, 46th SPI Reinforced Plastics/Composites Conference, 1991, paper 1B.
4. C. D. Han and K.-W. Lem, *J. Appl. Polym. Sci.*, **29**, 1879 (1984).
5. V. Bellenger, J. Verdu, M. Ganem, and B. Montaigne, *Polym. Polym. Compos.*, **2**, 9, 17 (1994).
6. M. Ganem, B. Montaigne, V. Bellenger, and J. Verdu, *J. Macromol. Sci., Pure Appl. Chem.*, **A30**(11), 829 (1993).
7. M. Ganem, E. La Fontaine, B. Montaigne, V. Bellenger, and J. Verdu, *J. Macromol. Sci. -Phys.*, **B33**, 155 (1994).
8. D. J. Herzog and T. B. Brown, *Mater. Perform.*, **33**, 30 (1990).
9. L. K. J. Tong and W. O. Kenyon, *J. Am. Chem. Soc.*, **69**, 1402 (1947).
10. H.J. Sawada, *J. Macromol. Sci.*, **C3**, 313 (1991).
11. M. Suzuki, H. Miyama, and S. Fujimoto, *J. Polym. Sci.*, **31**, 212 (1958).

12. K. Uno, M. Makita, S. Ooi, and Y. Iwakura, *J. Polym. Sci., Part A-1*, **6**, 257 (1968).
13. P. J. Flory, *Principles of Polymer Science*, Cornell University Press, Ithaca, NY, 1953.
14. V. R. Kamath and R. B. Gallagher, in *Developments in Reinforced Plastics*, Vol. 1, G. Pritchard, Ed., Applied Science Publishers, New York, 1980.
15. P. Beaunez, G. Helary, and G. Sauvet, *J. Polym. Sci., Part A: Polym. Chem.*, **32**, 1459 (1994).
16. A. Thomas, O. Jacyszyn, W. Schmitt, and J. Kolczynski, 32nd SPI Reinforced Plastics/Composites Conference, 1977, paper 3B.
17. E. Rizzardo (CSIRO Chemicals and Polymers), personal communication.
18. J. M. Salla, X. Ramis, J. L. Martin, and A. Cadenato, *Thermochim. Acta*, **134**, 126 (1988).
19. J. P. Cassoni, G. A. Harpell, P. C. Wang, and A. H. Zupa, 32nd SPI Reinforced Plastics/Composites Conference, 1977, paper 3E.
20. C. W. Macosko and D. R. Miller, *Macromolecules*, **9**, 199 (1976).
21. C. Walling, *J. Am. Chem. Soc.*, **67**, 441 (1945).
22. M. Avella, E. Martuscelli, and M. Mazzola, *J. Thermal Anal.*, **30**, 1359 (1985).
23. K. Horie, I. Mira, and H. Kambe, *J. Polym. Sci., A-1*, **8**, 2839 (1970).
24. K. Horie, I. Mita, and H. Kambe, *J. Polym. Sci., Part A-1*, **6**, 2663 (1968).
25. W. D. Cook, *J. Polym. Sci., Polym. Chem.*, **31**, 1053 (1992).
26. W. D. Cook, *Polymer*, **33**, 2159 (1992).
27. S. K. Soh and D. C. Sunderberg, *J. Polym. Sci., Polym. Chem.*, **20**, 1299, 1315, 1331 (1982).
28. G. T. Russell, D. H. Napper, and R. G. Gilbert, *Macromolecules*, **21**, 2141 (1988).
29. D. Verchere, H. Sautereau, J. P. Pascault, C. C. Riccardi, S. M. Moschiar, and R. J. J. Williams, *Macromolecules*, **23**, 725 (1990).
30. K. O'Driscoll and S. A. McArdle, *J. Polym. Sci.*, **60**, 557 (1959).
31. G. Wisanrakkit and J. K. Gillham, *J. Appl. Polym. Sci.*, **41**, 2885 (1990).
32. S. Montserrat, *J. Appl. Polym. Sci.*, **44**, 545 (1992).
33. E. F. Oleinik, *Adv. Polym. Sci.*, **80**, 49 (1986).
34. A. V. Tungare and G. C. Martin, *Polym. Eng. Sci.*, **33**, 614 (1993).
35. X. Peng and J. K. Gillham, *J. Appl. Polym. Sci.*, **30**, 4685 (1985).
36. J. G. Kloosterboer and G. F. C. M. Lijten, *Polymer*, **31**, 95 (1990).
37. J. D. Ferry, *Viscoelastic Properties of Polymers*, Wiley, New York, 1970.
38. P. G. Babayevsky and G. K. Gillham, *J. Polym. Sci.*, **17**, 2067 (1973); M. T. Aronhime and J. K. Gillham, *Adv. Polym. Sci.*, **78**, 83 (1986); G. Wisanrakkit, J. K. Gillham and J. B. Enns, *J. Appl. Polym. Sci.*, **41**, 1895 (1990).
39. I. Havlicek and K. Dusek, in *Crosslinked Epoxies*, B. Sedlacek and J. Kahovec, Eds., Walter de Gruyter & Co., New York, 1987, p. 417.
40. X. Wang and J. K. Gillham, *J. Appl. Polym. Sci.*, **45**, 2127 (1992).
41. S. L. Simon and J. K. Gillham, *J. Appl. Polym. Sci.*, **46**, 1245 (1992).
42. S. L. Simon and J. K. Gillham, *J. Appl. Polym. Sci.*, **47**, 461 (1993).
43. T. H. Grentzer, K. E. Kitchen, S. K. Lo, C. J. Spencer, and D. A. Rust, 45th SPI Reinforced Plastics/Composites Conference, 1990, paper 2B.
44. C. Feger and W. J. MacKnight, *Macromolecules*, **18**, 280 (1985).
45. J. P. Pascault and R. J. J. Williams, *J. Polym. Sci., Part B: Polym. Phys.*, **28**, 85 (1990).